Optimizing the thermal performance of building envelopes for energy saving in underground office buildings in various climates of China

Optimizing the thermal performance of building envelopes for energy saving in underground office buildings in various climates of China

Luyang Shi[1], Huibo Zhang[2], Zongxin Li[3], Zhiwen Luo[4], Jing Liu[1, 5*]

[1]School of Municipal and Environmental Engineering, Harbin Institute of Technology, 202 Haihe Street, Nangang District, Harbin, China

[2]School of Naval Architecture, Ocean and Civil Engineering, Shanghai Jiao Tong University, 800 Dongchuan Road, Minhang District, Shanghai, China

[3]The Fourth Design and Research Institute, Headquarters of the General Staff Corps, Beijing, China

[4]School of the Built Environment, University of Reading, Reading, United Kingdom

[5]State Key Laboratory of Urban Water Resource and Environment, Harbin Institute of Technology, Harbin, China

[*]Corresponding author: Jing Liu

Address: School of Municipal and Environmental Engineering, Harbin Institute of Technology, No.73, Huanghe Road, Nangang District, Harbin 150000, China.

Tel./fax: +86 0451 8628 2123.

E-mail: liujinghit0@163.com

Abstract This article investigates the influence of the thermal performance of building envelopes on annual energy consumption in a ground-buried office building by means of the dynamic building energy simulation, aiming at offering reasonable guidelines for the energy efficient design of envelopes for underground office buildings in China. In this study, the accuracy of dealing with the thermal process for underground buildings by using the Designer's Energy Simulation Tool (DeST) is validated by measured data. The analyzed results show that the annual energy consumptions for this type of buildings vary significantly, and it is based on the value of the overall heat transfer coefficient (U-value) of the envelopes. Thus, it is necessary to optimize the U-value for underground buildings located in various climatic zones in China. With respect to the roof, an improvement in its thermal performance is significantly beneficial to the underground office building in terms of annual energy demand. With respect to the external walls, the optimized U-values completely change with the distribution of the climate zones. The recommended optimal values for various climate zones of China are also specified as design references for public office building in underground in terms of the building energy efficiency.

Keywords: Underground office buildings; Thermal performance; Optimization; China; DeST simulation

1 Introduction

In the view of the significant increases of the population in urban cities over recent decades, underground buildings have played an increasingly important role in the development and improvement of metropolises. A growing number of underground buildings, such as underground parking spaces, shopping malls, hospitals, railways, and office buildings, have been constructed as alternatives for urban area expansion in metropolises worldwide [1], and especially in China [2，3]. For instance, the total area of underground space in Beijing has reached 72.68 million m^2 with a noted annual increase of over 7.3 million m^2 based on published figures in August 2014 [2]. The development of underground buildings effectively relieves land utilization in these mega cities, and definitely provides more living space for urbanites [4, 5]. Moreover, compared to buildings built above the ground, underground buildings may exhibit increased advantages in terms of building energy efficiency and indoor climate owing to their better capacities for heat storage, heat stability, and smaller temperature variations [6, 7]. Therefore, underground buildings require lower heating and cooling loads, save more energy for residents, and improve urban sustainability [6, 7, and 8]. Many studies have demonstrated that underground buildings possess immense potential in reducing energy demands that can save more than 23% of energy in comparison with similar aboveground buildings [6, 9, 10, and 11]. It should be noted that the energy analysis of earth-sheltered domestic buildings situated in Poland showed that approximately 47%-80% reduction in the heating energy demand could be achieved by using various thickness of thermal insulation [6].

Recently, some researchers have attempted to study the energy performance of underground buildings using various research methods such as a two–dimensional transient finite element model (FEM) to investigate heat loss in a basement [12], a two–dimensional dynamic model of heat transfer through building envelopes using MATLAB [13], a combination of computer programs FlexPDE and EnergyPlus to simulate the heating and cooling energy demands in earth–sheltered buildings [6], a three–dimensional analysis of the thermal resistance of an external insulation system of a basement [13], a three-dimensional finite difference model (FDM) to verify the energy reduction potential of underground buildings [14], and an experimental analysis of indoor temperature variations related to ground layers in underground wine cellars [15]. All these experimental and simulated research studies indicate that the energy performance of underground buildings is determined by a wide variety of influential factors such as design typology, building function, HVAC systems, covering soil depth and type, thermal insulation, air infiltration [8]. In terms of design typology, contact surface area of building with the earth plays a key role in heat transfer. Overall, adopted methodologies have been more sophisticated as compared to conventional methodologies used for buildings above the ground. Additionally, these factors interact and change with different outdoor climates and indoor conditions [8, 16]. Among these factors, the building envelope is a factor that can be easily designed and optimized in the early design stages for energy efficiency.

In terms of building envelope features for aboveground buildings，an improvement in the thermal performance of the envelope, such as an increase in the thermal

89 insulation level, can effectively reduce heat loss, and the annual energy demands for
90 both heating and cooling [17, 18]. The efficiency requirements for building envelopes,
91 such as the assembly's maximum U-value (overall heat transfer coefficient), are
92 determined for building energy efficiency based on the ASHRAE Standards 90.1–
93 2016 [19] in America, and GB50189–2015 in China [20]. However, the heat transfer
94 through an underground building is completely different from that of a building that is
95 above the ground because the soil's thermal properties are treated as a thermal
96 reservoir for modulating interior temperatures [21]. Therefore, these standards
97 correspond to buildings built above the ground and might be not suitable for
98 underground buildings in which the thermal performance of the envelopes is designed
99 for energy efficiency.

100 In this context, several researchers have focused on the investigation of the
101 influence of the thermal performance of the envelopes on energy consumption with
102 respect to heating and cooling loads for underground buildings [11, 13, 22, and 23].
103 Krarti and Choi demonstrated that additional insulation is required at the corners, as
104 opposed to the middle section of the surface to minimize the heat loss for
105 underground buildings, and that insulation material should be close to the soil surface
106 [13]. Yuan et al. evaluated the effect of building materials on the temperature and heat
107 flux for envelopes in a basement, and indicated that the thermal conductivity of
108 building materials is an important factor in the heat transfer of the envelopes [22].
109 Dronkelaar stated that the energy performance is more significantly dependent on the
110 U-value of the constructions and the ventilation rates in certain colder climates [11].

Staniec and Nowak suggested that thinner thermal insulation, elicits a better cooling effect gained from the soil, whereas a thicker insulation leads to a smaller heating energy demand [6, 23]. These studies indicates that the thermal performance of the envelopes in an underground building is one of the most important design criteria to allow the best thermal comfort effect [8]. However, the relationships between the annual energy demand and the thermal performance of the envelopes in underground buildings might not be very accurate and explicit, especially with respect to various climatic zones. In general, outdoor climatic conditions have a slight influence on the indoor environment and energy demand for underground buildings in a short time. However, the long-term distribution of ground temperature is crucial in determining the energy demand, which is dependent on the climate and soil's thermal properties. Although the simulated analysis by Staniec and Nowak illustrated the influence of thermal insulation on heating and cooling loads, the combined effect of thermal performance of the envelope on the annual energy demand (including heating and cooling energy) has not been considered in their study. Furthermore, their simulation was only performed for Polish climate conditions, and thus, it may not be possible to apply their conclusions to various climates around the world.

On the other hand, China has a vast territory spanning five different climatic conditions [24]. Specifically, temperature waves of underground spaces differ in terms of values, amplitude, period, and phase displacement for various climatic zones. Therefore, the efficiency requirements of building envelopes in an underground building may vary significantly with changes in the climate. Hence, a reasonable and

formal guideline, or a standard listing the efficiency requirements, are necessary for underground building envelopes in various climates to provide a basis for the energy-saving design of the envelopes, which is currently lacking in China.

The aim of this study is to investigate the influence of the thermal performance of the envelopes on annual energy consumption for underground office buildings in various climatic zones of China, thereby allowing the determination of the optimized U-value for building envelopes (including the roof and the exterior wall), and introducing reasonable guidelines for the energy efficient design of underground building envelopes. First, a building energy simulation tool known as the Designer's Energy Simulation Tool (DeST) was presented in detail to deal with the thermal process for the underground building and the accuracy of DeST is also validated by measured data. Thus, DeST is used to calculating the hourly heating and cooling loads for ground-buried office buildings in this study to optimize the thermal performance of the insulation configurations of envelopes for various climatic zones in China, based on the annual energy consumption.

2 Methodology

This section is organized in four parts. Section 2.1 describes the details for simulating thermal process within underground buildings by means of DeST. Section 2.2 presents a prototype underground building model implemented in the DeST platform. Section 2.3 shows the classification of climate zones in China and lists the ten major Chinese cities selected for this simulation. The evaluation method of

154 calculating annual energy demand based on hourly heating and cooling loads is
155 summarized in Section 2.4.

156 **2.1 Simulation tool**

157 DeST is an effective building energy simulation tool that was developed by
158 Tsinghua University in 1989. To-this-date, numerous case analyses and theoretical
159 validations are performed, and as a result, DeST has become a widely-used platform
160 for calculating building thermal processes and for dynamic simulations of the
161 building's energy distribution. Specifically, DeST develops a graphical user interface
162 that is based on AutoCAD for all simulation processes to avoid additional modelling
163 work and information loss due to conversion [25].

164 In terms of energy performance, the most significant difference between an
165 underground building and an aboveground building is that all the building partitions
166 are in contact with soil, rather than atmosphere. Therefore, it is critical to determine
167 surrounding ground temperature and calculate the heat transfer process of
168 ground-coupled envelopes that are in contact with the earth for simulating an
169 underground building. Generally, heat transfer within ground-coupled envelope is
170 computed using numerical methods, such as FEM and FDM [12, 14]. However, these
171 models are excessively time-consuming for hourly simulations over the period of a
172 year [25].

173 In DeST simulation, the heat transfer process of ground-coupled envelopes (the
174 envelopes that are contact with the earth) is decomposed into three processes which

175 are controlled by ground-coupled envelope surface temperature, outdoor ground
176 surface temperature and temperature difference of ground-coupled envelope surfaces
177 [26]. The schematic diagram of heat transfer within ground-coupled envelopes is
178 presented in Fig.1. Outdoor ground surface temperature (OGST) is mainly determined
179 by above air temperature, absorbed solar radiation, long wave radiation with sky.
180 Ground-coupled envelope surface temperature is mainly determined by room air
181 temperature, long wave radiation with occupant, light, equipment and other inner
182 surface in the room. Temperature of deep soil surface is set as constant and
183 approximately equals to mean ground surface temperature (MGST).

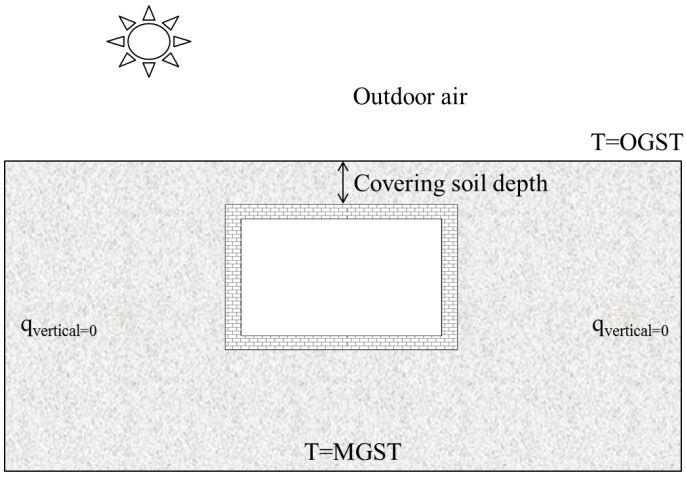

184

185 Fig.1 Schematic program of underground building's heat transfer and boundary condition (not in scale)

186 In the first process, outdoor ground surface temperature is set as zero and the
187 temperature of other ground-coupled envelopes is set the same as the selected one.
188 The heat transfer process controlled by ground-coupled envelope surface temperature
189 is computed by one-dimensional Equivalent Slab. In the second process, temperature
190 of all ground-coupled envelope surfaces is set as zero and outdoor ground surface
191 temperature is simplified as a constant and 1 year period harmonic variable. In the

192 third process, outdoor ground surface temperature is set as zero and the temperatures
193 of ground-coupled envelopes are different. The heat between ground-coupled
194 envelopes is exchanged through the soil and is computed by a one-dimensional Extra
195 Partition Wall. Therefore, replace the ground-coupled envelope in a room using
196 Equivalent Slab and treat the heat flux computed in the second and third process as
197 heat source of Equivalent Slab inner surface, and thus the heat transfer of
198 ground-coupled envelope is calculated and implemented into building thermal
199 simulation. This approach can save a large amount of time for the full-year calculation
200 compared with other numerical methods [26].

201 **2.2 Underground office building details**

202 All simulation stages are performed in DeST for a simplified prototype building
203 model based on a typical large-scale office building that is fully underground. The
204 building is located at a depth of 1.0 m below the ground in Beijing and has only one
205 underground floor with a story height of 3.3 m. The building is consisted of five
206 sections as detailed in a previous study [27]. Fig.2 shows the layout of the eastern
207 section of the building as the chosen prototype building model in the calculation,
208 which has a building area of 215.5 m^2. Table 1 lists the components and thermal
209 performance of the building envelope. The building is surrounded by rammed clay
210 that is considered as a special component for the exterior walls. The thermal
211 conductivity coefficient of rammed clay is 1.16 W/(m·K).

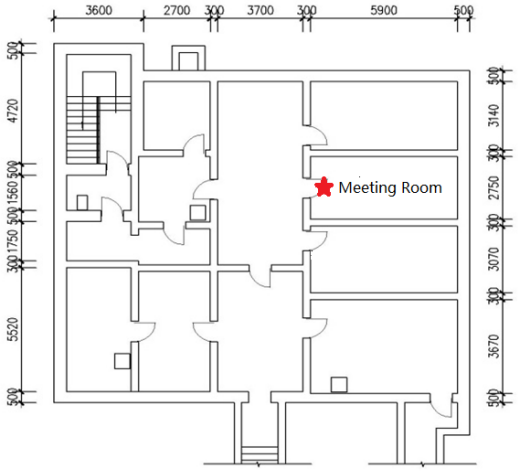

Fig.2 The layout of the simplified underground building (unit: mm)

Table 1 Components and the thermal performance of the building envelope

Building envelope	Building envelope components	U-value ($W/m^2 \cdot K$)
Roof	20 mm Lime mortar + 300 mm reinforced concrete	0.81
External walls	30 mm Lime mortar + 200 mm reinforced concrete	1.00

In this simulation, the layout and building structure are constructed using model parameters that are as close as possible to the real-life situation [28]. It is assumed that there is no infiltration or solar gains for the underground building because the building is completely buried beneath the surface.

Three scenarios are considered in the simulation. The details of building characteristics for the three scenarios are presented in Table 2. Scenario A is performed to simulate annual indoor temperature variations in the meeting room as depicted in Fig.2. Scenarios B and C are both executed to calculate the hourly load of the underground building. First, Scenario B is performed to investigate the influence of the U-value of the roof on the annual energy demand, and to determine its optimal U-value. This is followed by the execution of Scenario C to optimize the thermal

performance of the exterior walls. It should be noted that the U-value of the roof for Scenario C is adopted based on the optimized results in Scenario B. In this study, two covering soil depths (1.0 m and 3.0 m) （calculated between the rooftop of the building and the ground surface） are chosen because the depth also greatly affects the indoor heat environment of the subsurface structure [8]. In this simulation, the research objective is the public office building, thus the parameters of the thermal disturbances (Table 3) from the occupants, illumination, and equipment in the building are assumed to be the same as those of public buildings above the ground according to Chinese national standard for public buildings [20], which is typical and representative for office buildings. The schedules for the interior heat sources are described in Table 4. Mechanical ventilation does not consider the impact of fresh air on the heat transfer between the building and surrounding envelopes. Therefore, the fresh air load is not included in the simulation for the calculation of the annual hourly load.

Table 2 Building characteristics for the three executed scenarios

Scenario	Depth (m)	U-value of the roof ($W/m^2 \cdot K$)	U-value of the exterior wall and floor($W/m^2 \cdot K$)	Internal heat gains
A	3.0	0.81	1.00	None
B	1.0/3.0	Variable value	1.00	See Table 3
C	1.0/3.0	Optimal value	Variable value	See Table 3

Notes: Variable values: 0.22/0.49/0.81/1.00/1.50/2.00/2.45/2.97, optimal value: the optimized results of U-value for the roof in Scenario B.

Table 3 Internal heat sources for an underground building

Building function	MNP($people/m^2$)	MI(W/m^2)	MHGFE (W/m^2)

Public office	0.1	9.0	15

Notes: MNP: maximum number of individuals, MI: maximum illumination, MHGFE: maximum heat gain from the equipment.

Table 4 Schedules for various internal heat sources

Interior disturbance	Schedule
Occupants	ON from 08:00 to 17:00 on workday, OFF at all other times
Illumination	ON from 08:00 to 17:00 on workday, OFF at all other times
Equipment	ON from 08:00 to 17:00 on workday, OFF at all other times

For Scenarios B and C, the heating and cooling systems have considered the provision of a comfortable indoor environment in an underground building. The high heat storage capacity of the surrounding soil results in an indoor underground temperature that is lower than 20 °C sometimes even during the summer [15, 27]，and it is then necessary to heat the room. Thus, it is not suitable to simply set the same parameters for an underground space to those used for indoor air conditioning for buildings above the ground, such as 26 °C in the summer, and 20 °C in winter. In the simulation, the indoor temperatures of an underground building in the summer and winter were set to a wide range of temperatures that approximately spanned 20-28 °C, and 18-22 °C, respectively.

2.3 Climatic zones in China

Based on the different climatic characteristics, China is divided into five major climate zones as follows: a severe cold zone (SCZ), a cold zone (CZ), a hot summer and cold winter zone (HSCWZ), a hot summer and warm winter zone (HSWWZ), and a temperate zone (TZ) (Fig.3). This climatic classification framework is principally

based on the average temperatures in the coldest and hottest months [18].

Fig.3 Classification of climate zones in China and geographic locations of the 10 major cities selected for this study, as denoted by the red stars

For Scenario B and C, 10 typical cities covering the climate zones are selected for the investigation, and they are denoted using red stars, as shown in Fig.3. They represent the corresponding climatic zones. The meteorological data for these cities during a typical meteorological year is determined based on a multiyear weather database file [16]. In DeST, hourly data of weather variations is calculated in a similar manner to the calculation of the weather input parameters for Scenario B and C.

2.4 Annual energy demand calculation

The hourly heating and cooling loads for the underground building are obtained based on the calculations of Scenario B and C. The grades of energy used in the heating and cooling systems as well as their energy efficiencies are different. It is necessary to convert the various energy forms to electricity power by using the

277 method detailed in the GB50189–2015 Standard [20], and thus annual energy
278 consumption for underground building is obtained.

279 For all the climatic zones, space cooling is provided using water–cooled
280 centrifugal chillers [20], and the electricity consumption for cooling can be calculated
281 in accordance to Eq.(1):

282 $$E_C = \frac{Q_C}{A \times SCOP_T} \quad (1)$$

283 where, Q_C denotes the accumulative cooling load on the calculated DeST results in
284 kWh, A denotes the total cooling areas in m^2, and $SCOP_T$ is the synthetic coefficient
285 of performance for the cooling system and equals to 2.5 [20].

286 The heating system is determined based on the climate zones. The system
287 operation with a coal-fired boiler is applied in the SCZ and CZ, while the system that
288 operated with a natural-gas-fired boiler is applied in all the other climate zones [23].
289 The electricity consumption for the heating system can be evaluated using Eqs.(2) and
290 (3), respectively.

291 $$E_H = \frac{Q_H}{A\eta_1 q_1 q_2} \quad (2)$$

292 where, Q_H denotes the annual accumulative heating load based on the calculated
293 results of DeST in kWh, A denotes the total heating areas in m^2, η_1 denotes the
294 synthetic efficiency of the heating system with a coal–fired boiler and equals to 60%
295 [20], q_1 denotes the calorific value of standard coal and equals to 8.14 kWh/ kgce,
296 and q_2 denotes the coal consumption rate in the power generation and equals to
297 0.360 kgce/kWh.

298 $$E_H = \frac{Q_H}{A\eta_2 q_3 q_2}\varphi \quad (3)$$

Where, φ denotes the converted coefficient between standard coal and gas, and equals to 1.21 kgce /m^3, η_2 denotes the synthetic efficiency of the heating system with a natural gas–fired boiler and equals to 75% [20], and q_3 denotes the calorific value of gas and equals to 9.87 kWh/ kgce.

Finally, the annual energy consumption is the sum of E_H and E_C, and is considered as the evaluation index of the total energy consumption for a full year in this study.

3 Results and discussions

3.1 Analysis of room temperature simulation

Basal room temperature refers to the indoor temperature that arises from the thermal interaction between the outdoor climatic conditions and the building in its natural state [16]. In this case, there were no heating/cooling sources or working HVAC systems. In this study, the meeting room, denoted as a red star in Fig.2, was used as an example to analyse the indoor temperature variations throughout the entire year. Fig.4 (a) shows the measured indoor temperature data a period of 9–10 months, while the outdoor temperature variations of Beijing during the year at which tests were conducted are shown in Fig.4 (b). Additionally, the annual hourly basal room temperature of the meeting room was calculated using DeST (Scenario A), as presented in Fig.4 (a). It should be noted that the meteorological data for Scenario A were based on a weather database file that matched the year at which the tests were conducted.

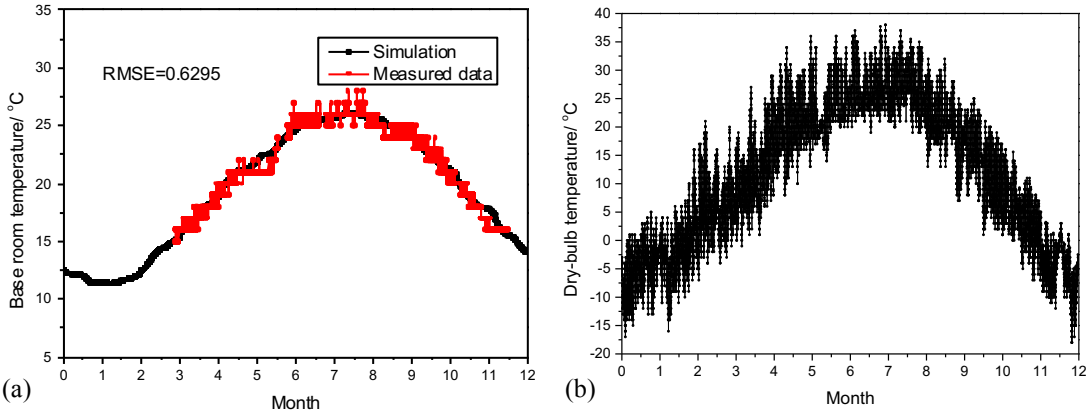

Fig.4 Basal temperature variations in the meeting room for simulation and measurements (a) and annual hourly dry-bulb temperature in Beijing during the testing year at which tests were conducted (b)

A sinusoidal behaviour of seasonal variability in the indoor temperature of the meeting room is distinctly observed in Fig.4. A comparison of the variations of indoor and outdoor temperatures indicates that their behaviours are almost identical in terms of the exhibited tendencies to monthly changes, but the temperature waves differ in terms of values, amplitude, and phase displacement [15]. First, the indoor temperature is very stable throughout the year eliciting a mean temperature of approximately 20 °C when compared to the outdoor temperature owing to the thermal inertia of the surrounding soil. The highest temperature of the underground space is approximately 10 °C lower than that of the outdoor air, while the lowest temperature of underground space is more than 20 °C larger than that of outdoor air. Additionally, the highest indoor temperature in underground buildings occurred in early August, while the highest outdoor temperature occurred in early July. Similarly, the lowest indoor temperature of the underground space is observed in mid-February, while the lowest outdoor temperature is observed in mid-January. This implies that the phase displacement between the indoor temperature in the underground space (at a depth of

1.0 m below the ground) and the outdoor temperature approximately corresponds to one month.

In order to compare the calculated and measured indoor temperature of the meeting room, we calculated the coefficient of variation of the root-mean square error (RMSE) using the following equation:

$$\mathrm{RMSE} = \sqrt{\sum_{i=1}^{N}(T_{meas} - T_{model})^2/N} \quad (4)$$

where, T_{meas} is the measured indoor temperature at a given time, T_{model} is the modelled indoor temperature at that same time, and *N* is the number of measurements.

The value of RMSE is used to quantify the agreements between measured and computational results and this value in Fig.4 (a) is 0.63, showing there is a good agreement between that experimental and computational results. Thus, the accuracy of the thermal process within underground buildings by means of DeST-based dynamic simulation is thus validated.

3.2 Analysis of hourly load for heating and cooling.

In this section, the calculated results for Scenario C are analyzed and illustrated as an example. In this case, the details of the simulation are as follows: the building is located at a depth of 1.0 m below the ground (Beijing), and the heat transfer coefficient of the roof is 0.8 W/(m^2·K). Fig.5 shows the simulation results for the distribution of annual hourly heating and cooling loads in an underground building.

In Fig.5, it is observed that the cooling load started at the end of July and lasted until the beginning of September, and this indicated that the cooling system worked during this period to regulate the indoor temperature to preset levels. The onset of the cooling operation occurred a month later than that used for buildings built above the ground. This may be owing to the phase displacement of the ground temperature compared to the outdoor temperature. A similar tendency in the heating load is also observed in Fig.5. For an underground building, the heating system mainly worked from January to February instead of the coldest months with respect to the outdoor atmosphere in Beijing (December and January).

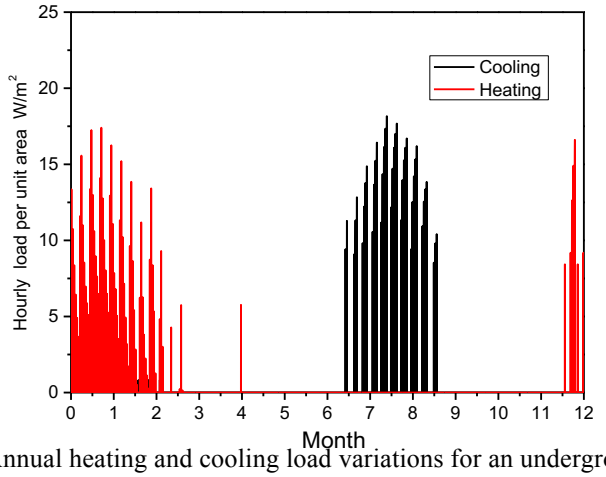

Fig.5 Annual heating and cooling load variations for an underground building

3.3 Impact of thermal characteristics of the roof on building energy demand

In this section, the influence of the thermal performance of the roof on the building's energy demand is analyzed for various climatic zones, based on the calculated results of Scenario B. Fig.6 (a)-(e) indicates that the annual energy demand changes as a function of the U-values of the roof for each of the corresponding climatic zones. As shown, the relationships between annual energy consumption and

U-values for the roofs for various climatic zones of China are very similar. Overall, the decrease in the U-values of the roof effectively reduced the building's energy demand by enhancing the thickness of the thermal insulation. This can be explained by the fact that the existing insulation diminished the impacts of the outdoor climate on the indoor environment of an underground space. For example, in Harbin (with a building depth of 1.0 m), the amount of annual energy consumption decreased from 6.20 $kW \cdot h/m^2$ to 3.55 $kW \cdot h/m^2$, and this corresponded to a change of approximately 42.7% when the U-value decreased from 2.0 $W/(m^2 \cdot K)$ to 0.5 $W/(m^2 \cdot K)$. The effectiveness of the U-value is more significant at lower values, while U-values higher than 2.5 $W/(m^2 \cdot K)$ minimized their impacts on the building's energy consumption.

Therefore, the analyzed results reveal that the energy efficiency requirements for the roofs of underground buildings are consistent with the standards for buildings above the ground. Thus, an improvement in the thermal performance of a roof, based on the increase of the insulation materials, is beneficial to the building's energy consumption. As shown in Fig.6 (a) and (b), it is also clear that additional insulation materials are required for cold climatic zones-and especially for SCZ to minimize heat loss through the roof, and especially for shallow-buried underground buildings.

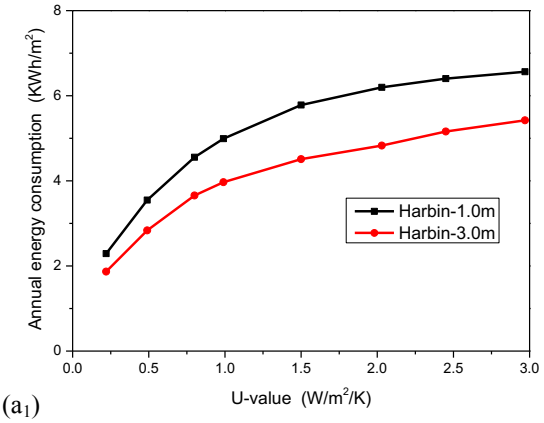

(a1)

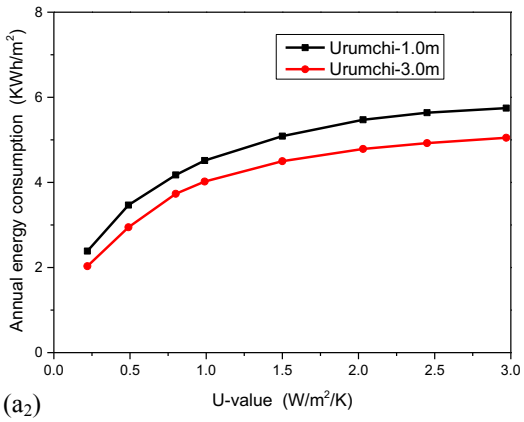

(a2)

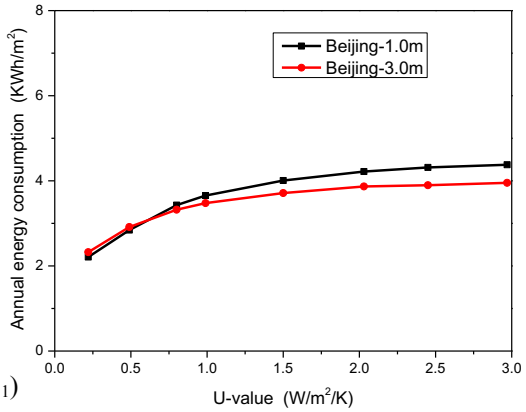

(b1)

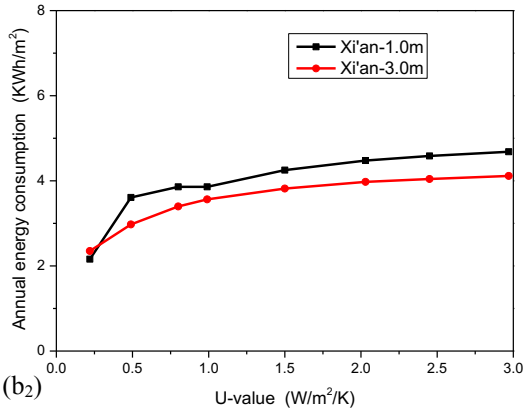

(b2)

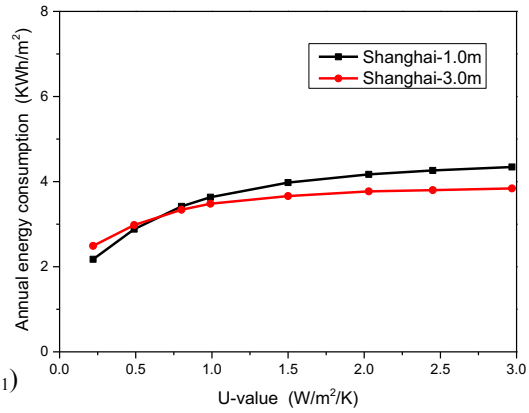

(c1)

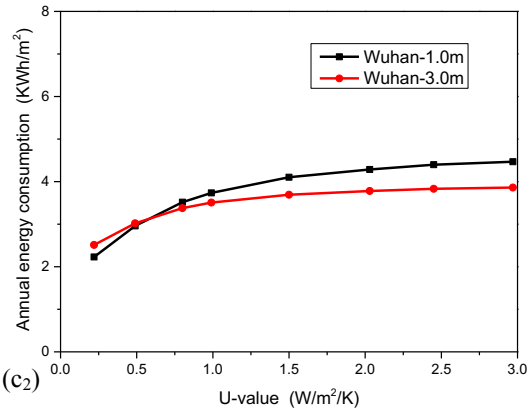

(c2)

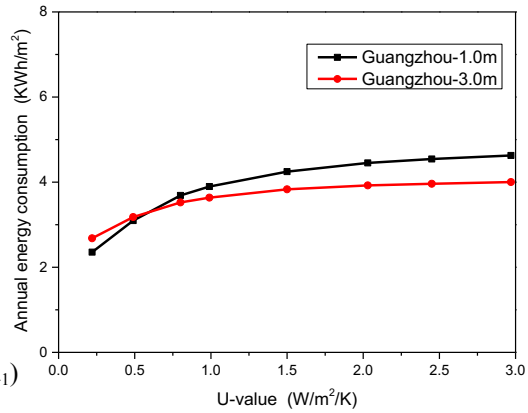

(d1)

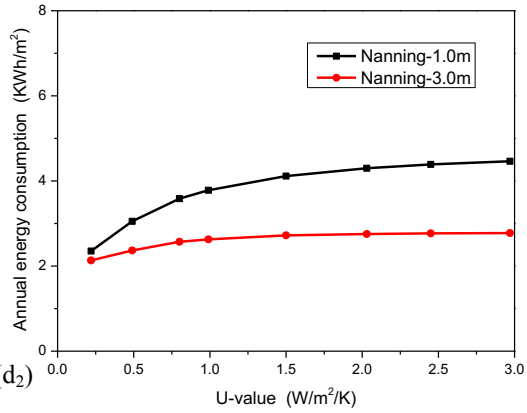

(d2)

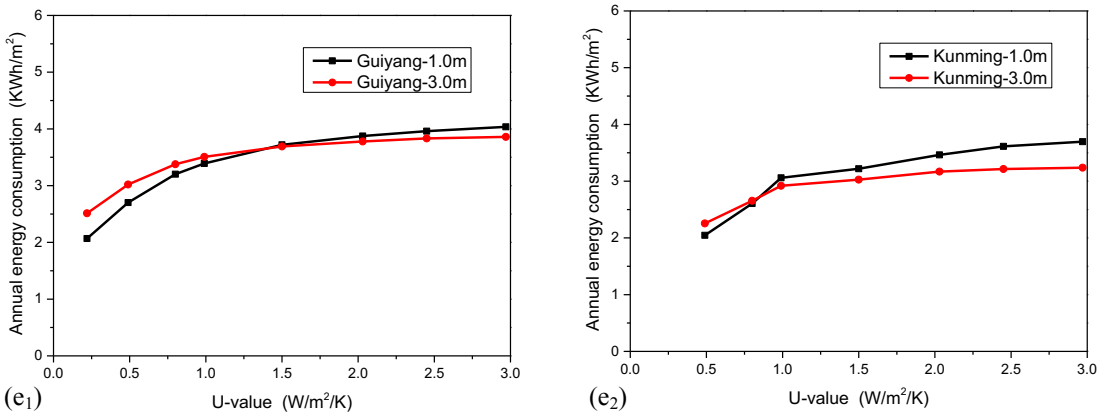

Fig.6 Relationships between annual energy demand and U-values of the roof for SCZ (a), CZ (b), HSCWZ (c), HSWWZ (d), and TZ (e)

3.4 Impact of the thermal characteristics of the exterior wall

Fig.7 (a)-(e) depicts the relationships between the annual energy demand and the U-values of the exterior wall in underground buildings for various climatic zones in China. Overall, these relationships vary with changes in the climate.

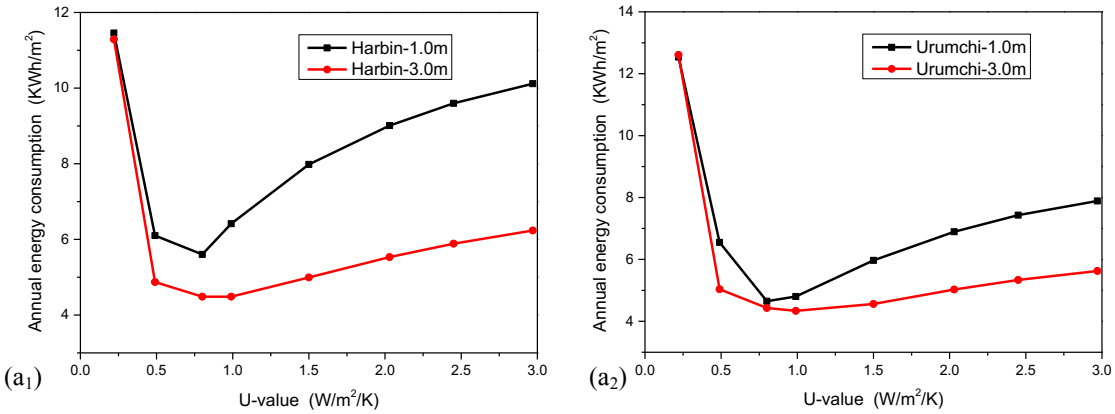

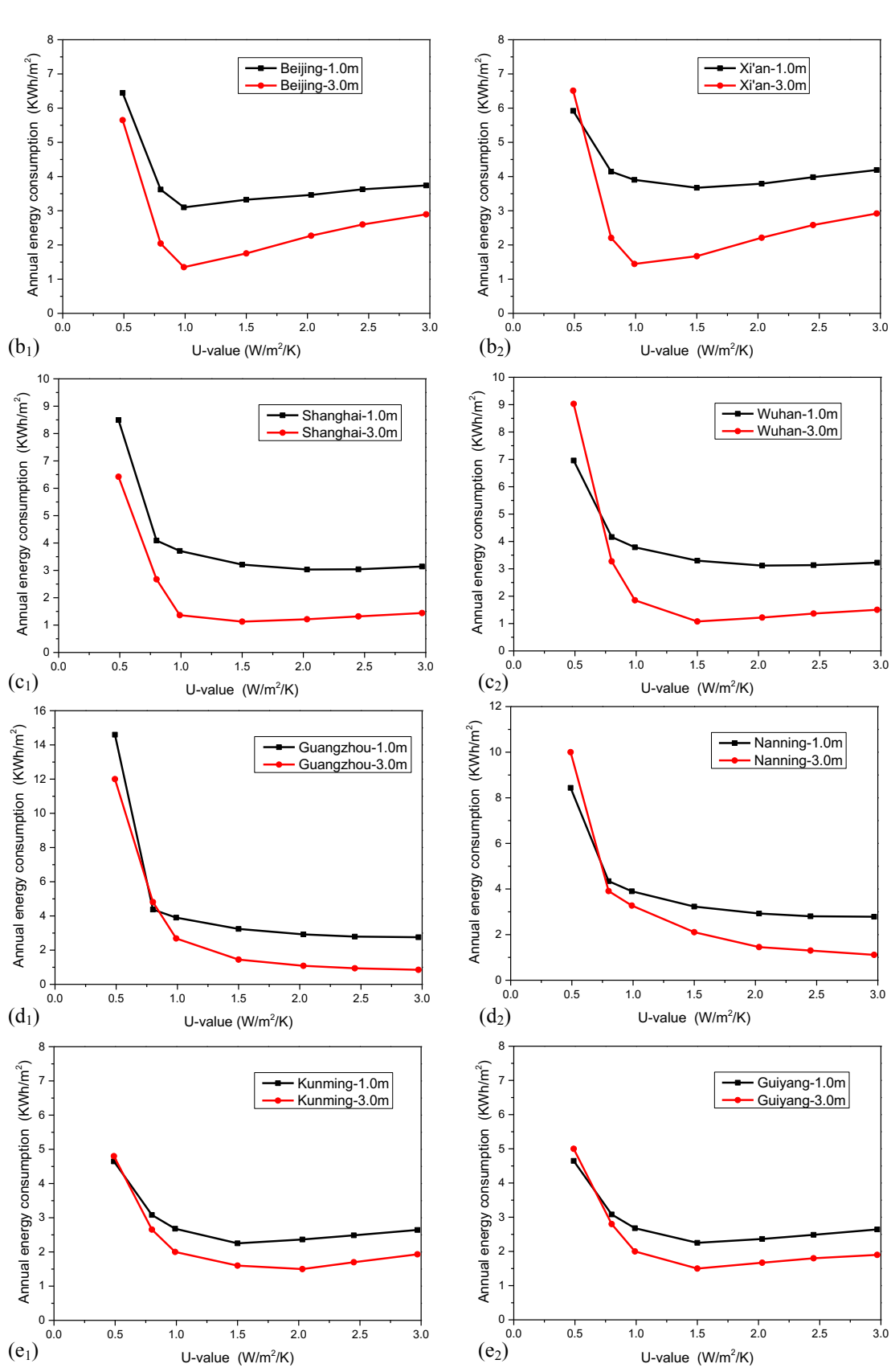

Fig.7 Relationships between annual energy demand and U-values of the exterior wall for SCZ (a), CZ

(b), HSCWZ (c), HSWWZ (d), and TZ (e)

A minimum is clearly observed in Fig.7 (a) and (b), thereby implying that there is an optimal U-value for the exterior wall for SCZ and CZ. With respect to SCZ, it is noted that increasing the U-value from 0.22 W/(m^2·K) to 0.8 W/(m^2·K) effectively reduces the annual energy consumption. However, this is followed by a continuous increase in the annual energy demand as a function of the U-value. Thus, the optimum U-value for the exterior wall for SCZ is approximately equal to 0.8 W/(m^2·K). Similarly, the optimum value of the exterior wall in an underground building for CZ is 1.0 W/(m^2·K).

The reason pertaining to the achieved optimal level of the U-value of the exterior wall is attributed to the differential impacts of energy consumption owing to heating and cooling. Fig.8 shows the variations in heating and cooling energies as a function of the U-values of the exterior wall in Harbin. Specifically, the thermal resistance of the exterior wall effectively prevents heat from being transferred into the surrounding soil in winter. Nevertheless, if the U-value is excessively low, the heat generated in the room cannot be effectively transferred into the soil, and this leads to an increased cooling load. In the summer, a decrease in the U-value of the exterior wall can effectively transfer more heat into the surrounding soil, and this is helpful in yielding significant decreases in the indoor temperature and in the cooling load. Thus, a decrease in the U-value of the exterior wall is beneficial in the reduction of the heating energy in winter, while an increase in the U-value is helpful in reducing the cooling energy in the summer. It is necessary to evaluate a trade-off by considering

the optimal annual energy consumption (including the heating and cooling energies) when the thermal performance of the exterior wall in an underground building is designed for energy conservation.

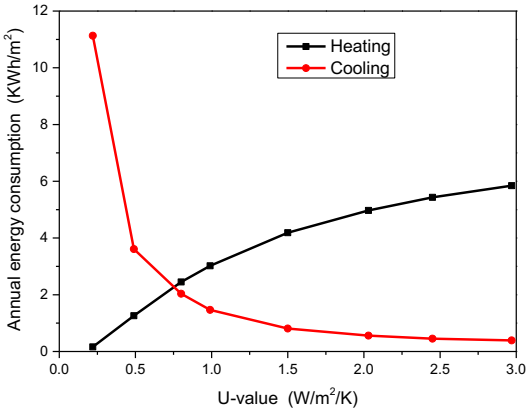

Fig.8 Variations in the annual energy consumption for heating and cooling as a function of U-values of the exterior wall in Harbin

With respect to the HSCWZ, the optimized value was approximately 1.5 W/(m^2·K), but when the U-value increased to 2.0 W/(m^2·K), its impact on building energy consumption was minimized. Similarly, the optimized U-value for TZ was approximately in the range of 1.5–2.0 W/(m^2·K), as shown in Fig.7 (e). It should be noted that higher U-values elicit lower annual energy demand for buildings in HSCWZ, even though the effectiveness of the U-value is not significant at higher values. This means that thermal insulation materials are not necessary for the exterior walls in underground buildings for HSCWZ, and that the U-value of the exterior walls should in general be larger than 2.0 W/(m^2·K). These findings are completely different from those for buildings above the ground. The main reason for this difference is the soil temperature. Fig.9 presents the measured data of the soil temperature at a depth of 3.2 m in a typical underground building in five selected

cities corresponding to different climatic zones in China [29].

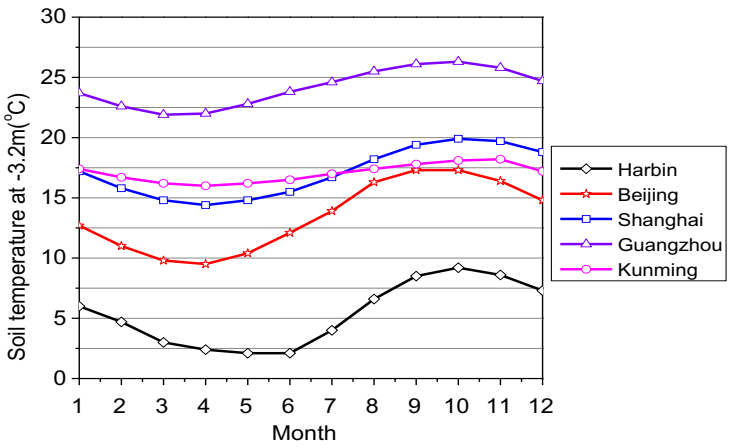

Fig. 9 Measured data of the soil temperature at a depth of 3.2 m below the ground

Based on Fig.9, it is observed that the average soil temperature corresponding to a depth of 3.2 m below the ground in Guangzhou (HSCWZ) reached 24 °C, and that the yearly dry-bulb temperature exceeded 20 °C. Thus, cooling of the interior space constitutes the main consequence in response to the climatic changes of HSWWZ. Increasing the U-value of the exterior wall is helpful in transferring the heat generated in the space into the surrounding soil.

Conversely, the fluctuation in the soil temperature in Harbin (SCZ) and Beijing (CZ) exceeded the corresponding fluctuations for the other three cities. For example, in Harbin, the average soil temperature (at a depth of 3.2 m below the ground) is the lowest among all the studied cities, and corresponded to approximately 5 °C. Thus, it is curial to reduce heat losses through the external walls. This is the reason why the basic requirements of good thermal insulation of the envelope need to be met for SCZ and CZ.

4 Conclusions

The focus of the present study is the thermal performance of the envelope for soil-buried office buildings, which may show distinct characteristics when compared to conventional buildings that are built above the ground. An advanced building energy-modelling tool (DeST) that accounted for the impact of the surrounding soil environment was used to simulate the building's energy performance in the case of a prototype underground building. The simulation results of the indoor air temperature for an underground meeting room were compared with the onsite long-term measurement data, and yielded a good agreement, thus demonstrating that dealing with the thermal process of an underground building using DeST is accurate and feasible. Most importantly, the hourly heating and cooling loads were calculated by DeST, the relationships between the annual energy consumption and the U-values of the envelopes were detected for various climates in China. The following conclusions can be drawn:

(1) The temperature waves between the indoor temperature of underground spaces and the outdoor climate differ in terms of values, amplitude, and phase displacement, owing to the high thermal capacity of the surrounding soil.

(2) Conversely, with respect to underground buildings, implementing a similar building energy efficiency strategy manifested by the decrease in the U-values of the envelopes (enhancing the thickness of thermal insulation), may result in an increased energy consumption when the thermal performance of the envelopes is designed for underground buildings.

(3) An improvement in the thermal performance of the roof plays an important role in reducing the energy demands for the underground office building. The energy efficiency requirements of roofs for the underground office buildings show consistency with the standard adopted for buildings that are above the ground

(4) The optimal U-values of an exterior wall for underground office buildings are completely different in the various climatic zones in China. For SCZ and CZ, the optimal U-values are 0.8 W/(m^2·K) and 1.0 W/(m^2·K), respectively, while for HSCWZ and TZ, the recommended optimal values are in the range of 1.5–2.0 W/(m^2·K). In terms of the building energy efficiency, thermal insulation is not required for HSWWZ.

These conclusions were drawn for soil-buried office buildings and the recommendations for optimal design U-values of building envelopes may not be suitable for other building functions. A further study should be carried out to investigate the impact of the thermal performance of building envelopes on annual energy consumption for various building functions, such as underground shopping malls, parking space, railways, hospitals, etc. In addition, the contact surface area of building with the earth plays a key role in heat transfer with underground buildings, and thus it is necessary to study the impact of contact surface area of building with the earth on the energy consumption and the optimal U-values of building envelopes, and further to correct these optimization results.

5 Acknowledgment

This study was financially supported by China Construction Engineering Design Group Corporation Limited (CSCEC–2014–Z–1–2).

6 References

[1] Nezhnikova E. The Use of Underground City Space for the Construction of Civil Residential Buildings [J]. Procedia Engineering, 2016, 165:1300-1304.

[2] Zhao JW, Peng FL, Wang TQ, et al. Advances in master planning of urban underground space (UUS) in China[J]. Tunnelling & Underground Space Technology Incorporating Trenchless Technology Research, 2016, 55:290-307.

[3] Yu RH, Ye QY. Review on the Development of Underground Shopping Mall in China[J]. Studies in Sociology of Science, 2012, 3(1).

[4] Shan M, Hwang BG, Wong KSN. A preliminary investigation of underground residential buildings: Advantages, disadvantages, and critical risks[J]. Tunnelling & Underground Space Technology, 2017, 70:19-29.

[5] He L, Song Y, Dai S, et al. Quantitative research on the capacity of urban underground space – The case of Shanghai, China[J]. Tunnelling & Underground Space Technology, 2012, 32(11):168-179.

[6] Staniec M, Nowak H. Analysis of the earth-sheltered buildings' heating and cooling energy demand depending on type of soil[J]. Archives of Civil & Mechanical Engineering, 2011, 11(1):221-235.

[7] Delmastro C, Lavagno E, Schranz L. Energy and underground[J]. Tunnelling &

599 Underground Space Technology Incorporating Trenchless Technology Research, 2016,
600 55(2925):96-102.
601 [8] Alkaff S A, Sim S C, Efzan M N E. A review of underground building towards
602 thermal energy efficiency and sustainable development[J]. Renewable & Sustainable
603 Energy Reviews, 2016, 60:692-713.
604 [9] Al-Mumin AA. Suitability of sunken courtyards in the desert climate of Kuwait[J].
605 Energy & Buildings, 2001, 33(2):103-111.
606 [10] Barker MB. Using the earth to save energy: Four underground buildings [J].
607 Tunnelling & Underground Space Technology Incorporating Trenchless Technology
608 Research, 1986, 1(1):59-65.
609 [11] Christian JE. Cooling season performance of an earth-sheltered office/dormitory
610 building in Oak Ridge, Tennessee[J]. Klinicheskaia Meditsina, 1984,
611 162(12):7049-7057.
612 [12] Wang F. Mathematical modeling and computer simulation of insulation systems
613 in below grade applications. Conference Thermal Performance of the Exterior
614 Envelopes of Buildings; 1979.
615 [13] Liu J, Jiang Y, Jin Y A. Dynamic Model of Heat Transfer through Underground
616 Building Envelope[C]// International Conference on Intelligent System Design and
617 Engineering Application. IEEE Computer Society, 2010:649-652.
618 [14] Choi S, Krarti M. Thermally optimal insulation distribution for underground
619 structures[J]. Energy & Buildings, 2000, 32(3):251-265.
620 [15] Tinti F, Barbaresi A, Benni S, et al. Experimental analysis of shallow

underground temperature for the assessment of energy efficiency potential of underground wine cellars[J]. Energy & Buildings, 2014, 80:451-460.

[16] Peng C, Wang L, Zhang X. DeST-based dynamic simulation and energy efficiency retrofit analysis of commercial buildings in the hot summer/cold winter zone of China: A case in Nanjing[J]. Energy & Buildings, 2014, 78(4):123-131.

[17] Nielsen TR. Simple tool to evaluate energy demand and indoor environment in the early stages of building design[J]. Solar Energy, 2005, 78(1):73-83.

[18] Lin YH, Tsai KT, Lin MD, et al. Design optimization of office building envelope configurations for energy conservation[J]. Applied Energy, 2016, 171:336-346.

[19] ASHRAE, ANSI/ASHRAE Standard 90.1—2010: Energy Standard for Building except Low-rise Residential Buildings, ASHRAE, Atlanta, GA, 2010.

[20] Design Standard for Energy Efficiency of Public Buildings. China Architecture and Building Press; 2015.

[21] Ma X, Cheng B, Peng G, et al. A numerical simulation of transient heat flow in double layer wall sticking lining envelope of shallow earth sheltered buildings[C]// International Joint Conference on Computational Sciences and Optimization. IEEE, 2009:195-198.

[22]Yuan Y, Cheng B, Mao J, et al. Effect of the thermal conductivity of building materials on the steady-state thermal behavior of underground building envelopes[J]. Building & Environment, 2006, 41(3):330-335.

[23] Staniec M, Nowak H. Analysis of the energy performance of –earth-sheltered houses with southern elevation exposed [J].

643 [24] Cui Y, Yan D, Hong T, et al. Comparison of typical year and multiyear building
644 simulations using a 55-year actual weather data set from China[J]. Applied Energy,
645 2017, 195.
646 [25] Yan D, Xia J, Tang W, et al. DeST — An integrated building simulation toolkit
647 Part I: Fundamentals[J]. Building Simulation, 2008, 1(2):95-110.
648 [26] Xie X, Jiang Y, Xia J. A new approach to compute heat transfer of
649 ground-coupled envelope in building thermal simulation software[J]. Energy &
650 Buildings, 2008, 40(4):476-485.
651 [27] Zhang H, Liu J, Li C, et al. Long-term investigation of moisture environment in
652 underground civil air defense work[J]. Indoor & Built Environment, 2016.
653 [28] Xie XN, Song FT, Zhang XL, et al. Building environment design simulation
654 software DeST (11): treatment of dynamic heat transfer through underground zone[J].
655 Heating Ventilating & Air Conditioning. 2005, 35(6):55-63.
656 [29] Organization of Chinese Architecture Standards Design Institute. Design manual
657 for air defense basement: HVAC[M].2006.